

In-situ Electron Microscopy Mechanical Testing for Steels

Shunsuke TANIGUCHI* Gerhard DEHM

Abstract

This paper outlines the techniques of in-situ electron microscopy mechanical testing to investigate the mechanical properties of hierarchical and complicated microstructures in steels. Compression tests of a precipitation hardening steel in scanning electron microscopy and transmission electron microscopy are shown as examples of the in-situ testing. The techniques are useful to understand the mechanical behavior of micrometer and sub-micrometer specimens.

1. Introduction

To improve the strength, ductility, and other mechanical properties of steel materials, it is important to quantify multiscale microstructures, such as crystal grains, dislocations, and precipitates, and associate them with the properties. For instance, the strength is related to microstructural factors including solute atoms, precipitates, dislocations, and crystal grains, as in solute strengthening, precipitation/particle hardening, dislocation hardening, and grain refinement strengthening. However, every steel has a hierarchical multiphase structures containing e.g. ferrite, martensite, bainite, pearlite, and austenite, where all the above-mentioned microstructural factors are contained. Many research studies have been conducted to clarify not only the strengthening mechanism in each substructure, but also the superposition of their strength contribution in a material.

Quantifying hierarchical microstructures requires a technique to observe them on their own spatial scales. Various analytical techniques, such as atom probe tomography, transmission electron microscopy (TEM), scanning electron microscopy (SEM), optical microscopy, and serial sectioning method, are used to perform multi-scale analysis of the microstructures, from atomic levels (10^{-10} m) for solid solution and segregation to the 10^{-4} m level for the distribution and shapes of the structures. Contrary to this, conventional mechanical tests mainly use test samples from 10^{-3} m to 10^{-2} m in size. They contain all microstructures length scales. It is difficult to discuss the contribution of an individual microstructural component to the global mechanical properties. It is necessary to miniaturize the mechanical test as well as the test samples to extract the mechanical property of an individual microstructural component.

Miniaturized mechanical tests need tiny test pieces. Samples such as wires, whiskers, and vapor-deposited films that are originally made minute in size have been used.¹⁻³⁾ It had been difficult to take a part out from a bulk material and extract microstructures into tiny

samples. This situation was changed by the development of focused ion beam (FIB) machining systems, which were invented in the 1970s, as a tool for the microelectronic industry. A FIB machining system is used to process a specific location in a scanning ion microscopy (SIM) image of the structure in a material. Use of this system makes it nowadays possible to extract a tiny piece from a specific material position.⁴⁾ Mechanical tests using test pieces between 10^{-6} m and 10^{-5} m in size have been reported; these tests were conducted to measure bending, tensile, and compression properties.⁴⁻⁶⁾ Tensile and compression tests using 10^{-7} m test pieces have been reported as well.^{7,8)}

As examples of applying mechanical tests using microscopic samples to steel materials, the following cases have been reported: Kumar et al. reported an approach to predict the deformation behavior of macroscopic test pieces using the crystal plasticity finite element method, by extracting the stress-strain response of each of ferrite and martensite in transformation induced plasticity (TRIP) steel and dual phase (DP) steel through micro-pillar compression testing.⁹⁻¹¹⁾ Xie et al. investigated the influence of dislocations and their clustering in Nb-microalloyed steel on the mechanical properties by *in-situ* TEM compression testing.¹²⁾

Nippon Steel & Sumitomo Metal Corporation has employed indenter systems in SEM and TEM in order to associate hierarchical microstructures with mechanical properties by conducting microscopic mechanical tests. In order to apply them to steel materials, we have been working to establish test piece processing conditions and mechanical test conditions. *In-situ* SEM mechanical testing is expected to allow for evaluation of the deformation behavior in a single crystal, the inhomogeneous deformation behavior of structures such as ferrite and martensite, and the inhomogeneous deformation at grain boundaries and within grains. The *in-situ* TEM mechanical testing that we consider allows for testing even smaller test

* Researcher, Materials Characterization Research Lab., Advanced Technology Research Laboratories
1-8 Fuso-cho, Amagasaki City, Hyogo Pref. 660-0891

objects than those used for SEM, and also for observing deformation behavior and dislocations inside a material when sufficiently thin samples are used. This paper presents examples of *in-situ* SEM and TEM compression testing applied to precipitation hardening steel.

2. In-situ SEM Compression Test

The sample used for the test was precipitation hardening steel with TiC particles of approx. 7 nm in equivalent sphere diameter. The TiC particles precipitate in ferrite at intervals of approx. 114 nm on a slip plane. The ferrite had a body centered cubic (BCC) structure. The chemical composition of the precipitation hardening steel was Fe-0.05C-0.50Mn-0.1Ti-2.96Al-0.0009N (mass%).¹³⁾ After the solution treatment, TiC precipitation treatment was isothermally performed at 660°C for 8 hours.

Using the electron backscatter diffraction (EBSD) method, the crystal orientation in the direction perpendicular to the polished surface was measured. Based on the results, the setup shown in Fig. 1 was used in the compression test such that the crystal orientation,

with which a single slip was anticipated, was set as the compression axis. Circular pillars were made using the FIB machining system. The current of Ga ion beams in the process was reduced in stages to 16 nA, 2 nA, and 240 pA at an accelerating voltage of 30 kV. This was to sharpen the top surface edges of the circular pillars, while shortening the processing time.

The compression test was conducted in the displacement open-loop control mode at a strain rate of $10^{-3} s^{-1}$. Figure 2 shows an example of the compression test results. The compression test was conducted using circular pillars between approx. 1000 nm to approx. 2500 nm in diameter. While the circular pillars of between approx. 1500 nm to approx. 2500 nm in diameter had two active slip systems, the circular pillars of approx. 1000 nm diameter had one active slip system. Nominal stress was calculated by dividing the measured load by the area at the center in the circular pillar height direction, and nominal strain was also obtained by dividing the displacement by the circular pillar height. Figure 2c) shows the stress measured for 1559 nm and 2583 nm pillars which were repeatedly unloaded and reloaded to prevent bending of the pillars by lateral

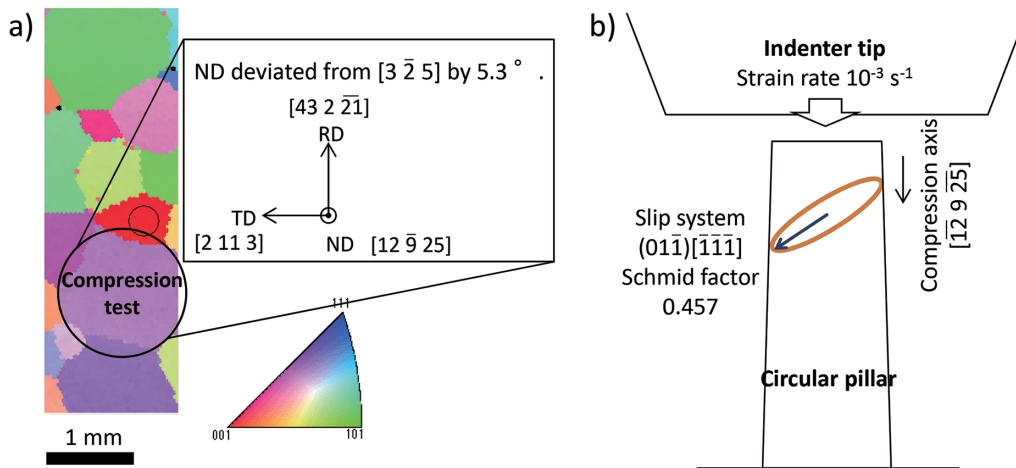


Fig. 1 Settings of compression test
 a) A grain where pillars were fabricated, b) Conditions of compression test and a slip system which would be activated

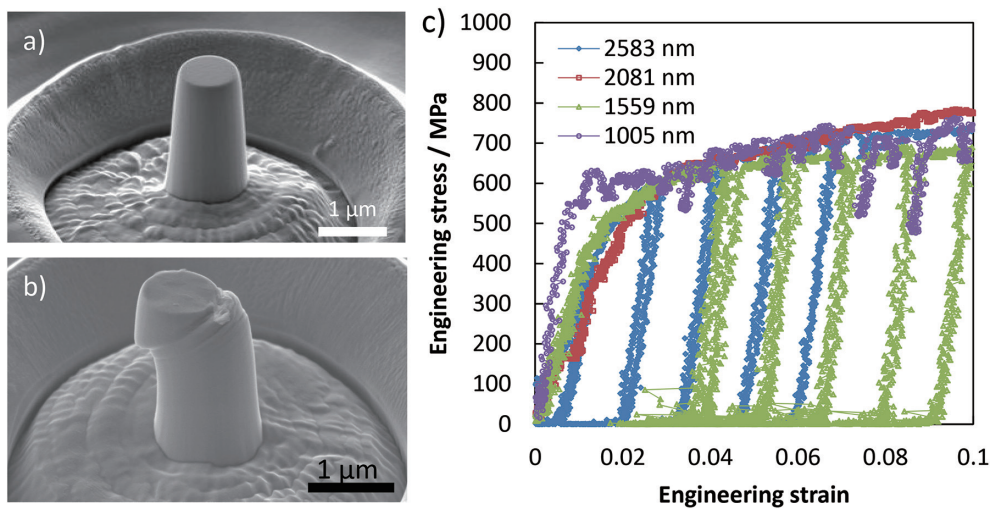


Fig. 2 Examples of *in-situ* compression test in SEM
 a) A SEM image of a pillar before compression, b) A SEM image of a pillar after compression, c) Engineering stress and strain curves of compression tests in SEM

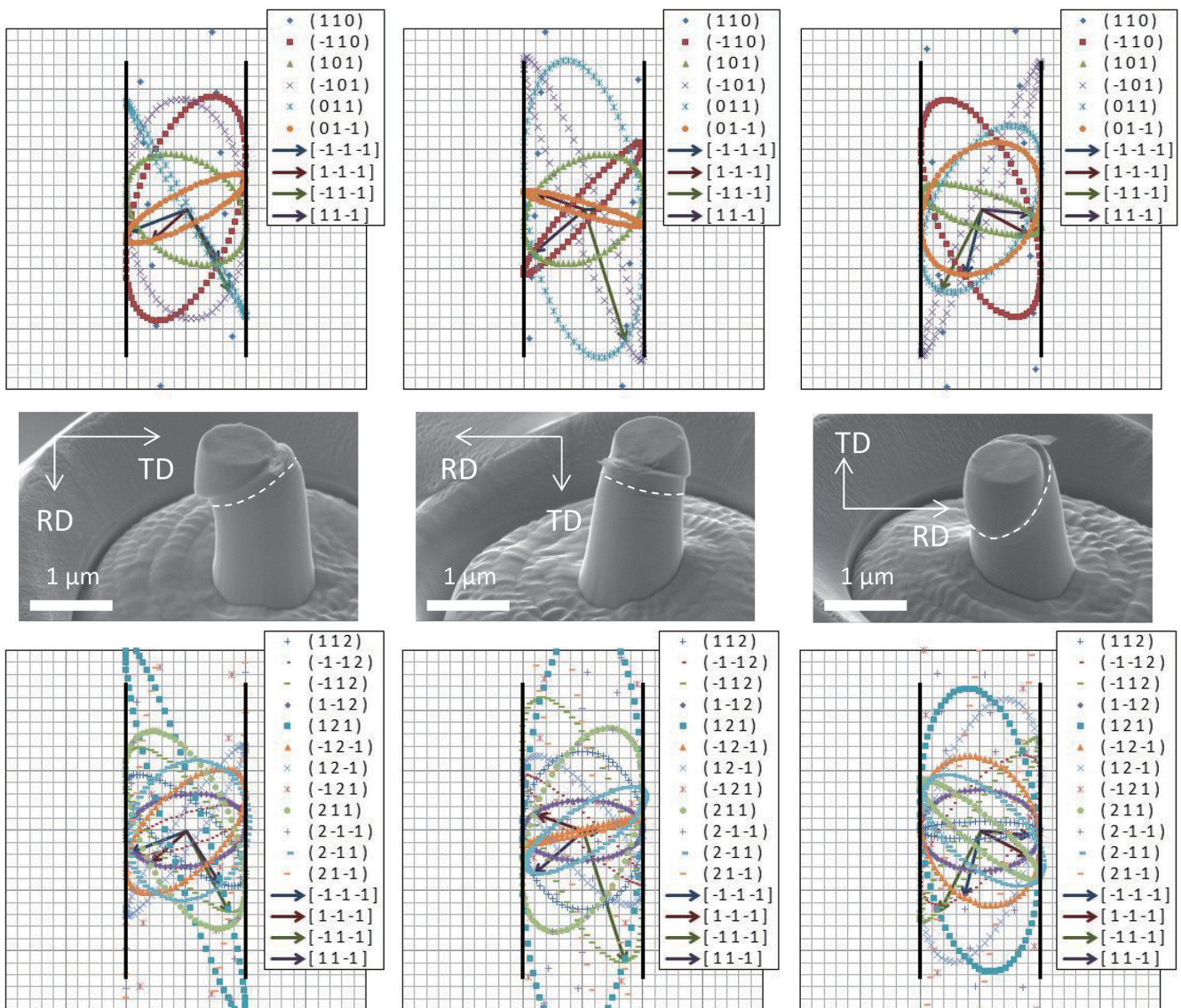


Fig. 3 Analysis of slip system of circular pillar

frictional forces. After obtaining the average value by taking further pillar sizes into account, no dependency of the flow stress on the pillar diameter was observed.

The activated slip systems were determined by comparing the observed slip lines and slip direction of each circular pillar with the calculated ones. As shown in Fig. 3, the slip lines and slip directions in the $\{110\}\langle 111\rangle$ and $\{112\}\langle 111\rangle$ slip systems were predicted. Each pillar was observed from several directions in SEM. Then it was found that the slip system of $(01\bar{1})[\bar{1}\bar{1}\bar{1}]$ with the largest Schmid factor was activated in pillars with a single active slip system, while the slip systems of $(01\bar{1})[\bar{1}\bar{1}\bar{1}]$ and $(101)[11\bar{1}]$ were activated in pillars with two active slip systems.

Rogne et al. reported the dependency of flow stress on the size in pure iron. The flow stress of pure iron decreased when the micro-pillar diameter was between approx. 100 nm and approx. 4000 nm.¹⁴⁾ In our test, the flow stress was almost constant with the micro-pillar diameters between approx. 1000 nm to approx. 2500 nm. This suggests that precipitates in ferrite inhibit the dislocation motion, and that the interaction between precipitates and dislocations

(precipitation hardening) dominate the plastic deformation for the studied circular pillar diameters. It has been confirmed by our test, by micropillar experiments reported in literature of oxide dispersion strengthened Ni-based superalloy¹⁵⁾ and Cu with damage from proton beam irradiation¹⁶⁾, the flow stress stays at a constant flow stress value nearly equal to the flow stress of these materials in the form of a bulk, when the sample diameters exceed a certain value. It is considered that in the case of a steel system as well, for a pillar in which the dislocation motion is blocked by something, the flow stress equivalent to that of the bulk of the steel can be expected when the pillar has a diameter up to a certain value.

3. In-situ TEM Compression Test

The precipitation hardening steel used as the sample in the above-described *in-situ* SEM compression test was used for *in-situ* TEM compressing testing. Circular pillars in diameter from approx. 100 nm to approx. 1000 nm were formed through the FIB machining system. They were processed using a Ga ion beam at an accelerating voltage of 30 kV and current of 120 pA, and then finished us-

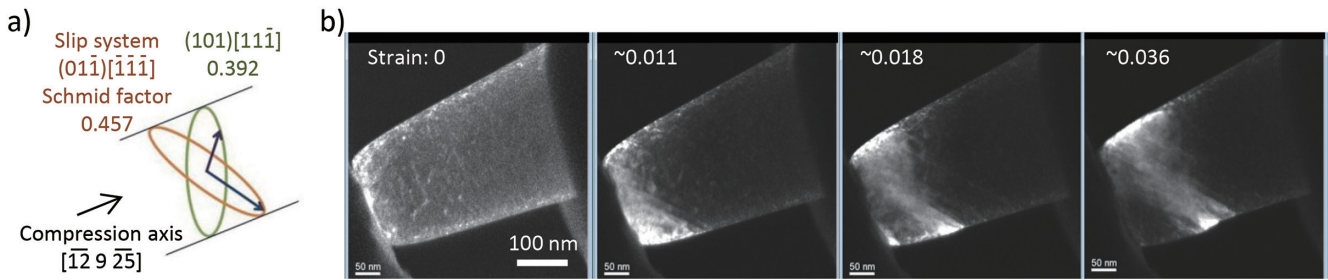


Fig. 5 Deformation behavior during compression test in TEM

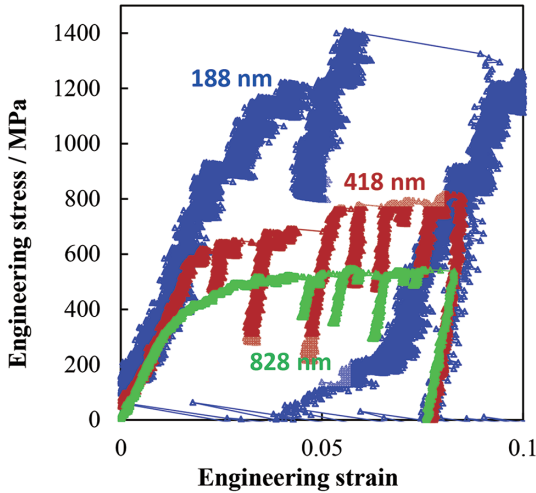


Fig. 4 Engineering stress and strain curves of compression test in TEM

ing a 20-pA beam. The compression test was conducted in the displacement closed-loop control mode at a strain rate of 10^{-3}s^{-1} . The conversion of the load-displacement relationship into the nominal stress-nominal strain relationship was the same as for the *in-situ* SEM compression test.

Figure 4 is an example of nominal stress-nominal strain curves obtained from the *in-situ* TEM compression test. As the diameter becomes smaller, the flow stress increases, and sudden stress drops called strain burst, in the stress-strain curves recorded in the displacement control mode become larger. As a result of *in-situ* SEM and TEM compression tests on 37 circular pillars, the flow stress was almost constant on average when the diameter was larger than approx. 330 nm, and had a power law dependency on the diameter for pillars smaller than approx. 330 nm in diameter; thus, the tests revealed that the flow stress dependency on the pillar diameter changes.

Figure 5 shows the deformation behavior during the *in-situ* TEM compression test. Figure 5a) illustrates the slip system observed in dark-field TEM images of Fig. 5b). As seen notably from the image of 0.018 strain, it seems that two slip systems having Schmid factors of maximum $(01\bar{1})[\bar{1}\bar{1}\bar{1}]$ and $(101)[11\bar{1}]$ were active. However, it was the $(01\bar{1})[\bar{1}\bar{1}\bar{1}]$ slip system, as seen in the image of 0.036 strain, that significantly deformed when further compression was applied. This is presumably because the deformed pillar became misaligned from the uniaxial compression position due to the tapered form of the pillars and the part in contact with the indenter

moved in the lower right direction of the images as deformation progressed.

As described above, *in-situ* TEM mechanical testing makes it possible to observe the slip behavior in pillars in a more detailed manner. However, since it is difficult to make a pillar small enough for an electron beam to penetrate well, quality images have not yet been obtained. Establishment of the specimen fabrication technique remains a challenge with Ga ion beam FIB milling.

4. Conclusion

This article describes examples of the application of *in-situ* SEM and TEM compression testing to precipitation hardening steel, with respect to *in-situ* electron microscopy mechanical testing technologies investigated by Nippon Steel & Sumitomo Metal as techniques to associate microstructures with mechanical properties. Our tests demonstrated that a material system that contains some obstacle to the dislocation motion and that is in a pillar with a diameter up to a certain value could have a flow stress equivalent to the bulk of the material. We also showed that *in-situ* TEM mechanical testing would allow slips in pillars to be observed in a more detailed manner. In the future, we expect that the techniques described here can be applied to various steel materials such as TRIP and DP steels, and utilized as tools to clarify relationships between hierarchical microstructures and mechanical properties.

Acknowledgements

Support by Dr. Christoph Kirchlechner, Dr. Rafael Soler, and Dr Christian Liebscher from the Max-Planck-Institut für Eisenforschung (Germany) is gratefully acknowledged.

References

- 1) Taylor, G.F.: Phys. Rev. 23, 655 (1924)
- 2) Brenner, S.S.: J. Appl. Phys. 27, 1484 (1956)
- 3) Neugebauer, C.A.: J. Appl. Phys. 31, 1096 (1960)
- 4) Uchic, M.D., Dimiduk, D.M.: Mater. Sci. Eng. A. 400–401, 268 (2005)
- 5) Jaya, B.N. et al.: J. Mater. Res. 30 (5), 686 (2015)
- 6) Kiener, D. et al.: Acta Mater. 56, 580 (2008)
- 7) Kiener, D. et al.: Adv. Eng. Mater. 14 (11), 960 (2012)
- 8) Kiener, D., Minor, A.M.: Acta Mater. 59, 1328 (2011)
- 9) Ghassemi-Armaki, H. et al.: Acta Mater. 61, 3640 (2013)
- 10) Ghassemi-Armaki, H. et al.: Acta Mater. 62, 197 (2014)
- 11) Srivastava, A. et al.: J. Mech. Phys. Solids. 78, 46 (2015)
- 12) Xie, K. Y. et al.: Acta Mater. 61, 439 (2013)
- 13) Kobayashi, Y. et al.: Scripta Mater. 67, 854 (2012)
- 14) Rogne, B.R.S., Thaulow, C.: Mater. Sci. Eng. A. 621, 133 (2015)
- 15) Girault, B. et al.: Adv. Eng. Mater. 12 (5), 385 (2010)
- 16) Kiener, D. et al.: Nat. Mater. 10, 608 (2011)

NIPPON STEEL & SUMITOMO METAL TECHNICAL REPORT No. 118 MARCH 2018



Shunsuke TANIGUCHI
Researcher
Materials Characterization Research Lab.
Advanced Technology Research Laboratories
1-8 Fuso-cho, Amagasaki City, Hyogo Pref. 660-0891



Gerhard DEHM
Director, PhD
Max-Planck-Institut für Eisenforschung GmbH